Comparative population genetics of habitat-forming octocorals in two marine protected areas: eco-evolutionary and management implications

Mathilde Horaud, Rosana Arizmendi-Meija, Elisabet Nebot-Colomer, Paula López-Sendino, Agostinho Antunes, Simon Dellicour, Frédérique Viard, Raphaël Leblois, Cristina Linares, Joaquim Garrabou, et al.

Conservation Genetics
https://doi.org/10.1007/s10592-023-01573-8

RESEARCH ARTICLE

Comparative population genetics of habitat-forming octocorals in two marine protected areas: eco-evolutionary and management implications

Mathilde Horaud[1,2] · Rosana Arizmendi-Meija[1] · Elisabet Nebot-Colomer[3] · Paula López-Sendino[1] · Agostinho Antunes[4,12] · Simon Dellicour[5,6] · Frédérique Viard[7,8] · Raphael Leblois[9] · Cristina Linares[10] · Joaquim Garrabou[1,11] · Jean-Baptiste Ledoux[1,4]

Received: 25 February 2023 / Accepted: 5 September 2023

Abstract

Current efforts to halt the decline of biodiversity are based primarily on protecting species richness. This narrow focus overlooks key components of biological diversity, particularly the infra-species genetic diversity, which is critical to consider with respect to genetic adaptation in changing environments. While comparative population genetics is recognized as a relevant approach to improve biodiversity management, it is still barely considered in practice. Here, a comparative population genetics study was conducted on two key habitat-forming octocoral species, *Corallium rubrum* and *Paramuricea clavata*, to contribute to management of two Marine Protected Areas (MPAs) in the northwestern Mediterranean. Contrasting patterns of genetic diversity and structure were observed in the two species, although they share many common biological features and live in similar habitats. Differential genetic drift effects induced by species-specific reproductive strategies and demographic histories most likely explain these differences. The translation of our results into management strategies supports the definition of four management units. We identified a coldspot of genetic diversity, with genetically isolated populations, and a hotspot of genetic diversity that has a central role in the system's connectivity. Interestingly, they corresponded to the most recent and the oldest protected areas, respectively. This case study shows how moving from a "species pattern" perspective to an "eco-evolutionary processes" perspective can help assess and contribute to the effectiveness of biodiversity management plans.

Keywords Mediterranean sea · Marine protected area · Habitat forming corals · Comparative population genetics · Conservation prioritization

Introduction

Global change is driving substantial marine biodiversity changes worldwide, altering the relationship between nature and people (Diaz et al. 2015), and resulting in detrimental social, cultural and economic consequences (IPBES, 2019; IPCC, 2021). The documented decline in biodiversity is unprecedented and calls for ambitious conservation efforts. The Convention on Biological Diversity (CBD) Aichi Target 11 (https://www.cbd.int/decision/cop/default.shtml?id=13365) was adopted to protect at least 10% of coastal and marine areas by 2020. This objective has not been reached (Claudet et al. 2020). However, the existing marine protected areas (MPAs) have already proved to benefit marine conservation (Magris et al. 2018), fisheries management (Gaines et al. 2010) and in some cases, to mitigate the impact of climate change (Alvarez-Romero et al. 2018). In addition, research dedicated to MPAs leaped forward, improving our abilities to design, manage and improve their functioning (Baskett and Barnett 2015).

Besides an effective enforcement, the benefits of MPAs rely on an accurate understanding of the processes shaping and maintaining biodiversity patterns (Sale et al. 2005).

JBL, PLS, CL belong to the research group MedRecover (https://medrecover.org) led by JG at the Institute of Marine Science (ICM-CSIC) in Barcelona, Spain. The group is focused on the conservation biology of Mediterranean rocky benthic communities and develops complementary approaches from population genetics to community ecology. JBL is affiliated to the Interdisciplinary Centre of Marine and Environmental Research (CIIMAR; http://CIIMAR.up.pt/) in Porto, Portugal.

Extended author information available on the last page of the article

Published online: 30 September 2023

Infra-specific genetic diversity is a pillar of biodiversity that enables natural populations' responses to environmental changes (Hoban et al. 2020; Figuerola et al. 2023). The spatial patterns of genetic diversity result from complex interactions between ecological and evolutionary processes (e.g., genetic drift, natural selection, reproduction; see Schoener 2011). These processes and their interactions are dynamic over space and time in response to historical and contemporary biotic (e.g., life history attributes) and abiotic factors (e.g., physical barriers). While crucial for effective management of biodiversity, their inferences remain quite challenging. In this regard, comparative population genetics among species with contrasting life histories across similar areas offers a robust framework, which can be used to improve MPAs management (e.g., Lukoschek et al. 2016). This is particularly true when it comes to the need to understand the spatial scale and drivers of connectivity within and among MPAs as well as between MPAs and neighboring unprotected areas (Magris et al. 2018). Yet, patterns of genetic diversity and underlying processes remain overlooked by biodiversity managers, potentially restricting the benefits of existing protected areas (Hoban et al. 2020).

The Mediterranean Sea is a striking example of the challenges faced when aiming to protect marine biodiversity. The Mediterranean is indeed both a hotspot of biological diversity (Coll et al. 2010) and a hotspot of anthropogenic pressures (Cramer et al. 2018). More than 1,100 MPAs, representing 6.5% of the sea surface, are reported in the Mediterranean but most of them are weakly enforced with only 76 (0.04% of the sea surface) fully protected areas (Claudet et al. 2020). Different studies addressed the potential benefits of these MPAs, yet mainly focused on a large geographic scale (i.e., whole Mediterranean basin) and particular taxa, notably commercial fishes (e.g., Blowes et al. 2019). In contrast, little is known about the functioning of those protected areas at a regional scale and for ecologically important species, such as habitat-forming species (but see Gazulla et al. 2021; Ledoux et al. 2021). Because they increase habitat complexity with positive effects on the associated community (Gómez-Gras et al. 2021), habitat-forming species are highly relevant targets in conservation biology (Palumbi 2009).

Here, we aim to demonstrate how comparative population genetics focused on ecologically key species can provide inputs for the management of protected area. As a case study, we focused on two habitat-forming octocorals, the red coral, *Corallium rubrum*, and the red gorgonian, *Paramuricea clavata* in two MPAs, the "Parc natural del Cap de Creus" and the "Parc natural Montgrí, les Illes Medes i Baix Ter," located 20 km apart on the Catalan coast, of the northwestern Mediterranean Sea. Both species are particularly relevant for biodiversity management, considering their role in providing structure for rich species diversity found in coralligenous communities (> 1,600 sp.; Ballesteros 2006). Based on an overlapping sampling (i.e. same localities), we: 1) characterized the patterns of spatial genetic diversity and structure in the two species, 2) inferred the levels of genetic isolation and 3) reconstructed the demographic history of each sampling site.

Material and methods

Case studies: marine protected areas and model species

The Parc natural del Montgrí, les Illes Medes i Baix Ter was established in 2010 with a marine part covering more than 2,000 ha. It includes a few kilometers of coastal area, the Montgrí coastal area (MCA) and the archipelago of the Medes Islands (MI). The archipelago was established as a marine reserve in 1983, with a 94-ha no-take reserve. The Parc Natural del Cap de Creus was established more recently, in 1998, covering almost 3,000 ha. We distinguished two different areas, the northern part of Cap de Creus (NPCC) and the southern part of Cap de Creus (SPCC) given their contrasting environmental conditions (Fig. 1). Contrasting management policies characterize the two MPAs. Around the Medes Islands, fishing is totally banned, while artisanal and recreational fishing are allowed in the Montgrí coastal area and in the Parc Natural del Cap de Creus. In addition, while diving is permitted in the two MPAs, the impact of recreational diving on biodiversity in the Medes Islands is a matter of concern (Linares et al. 2010).

The red coral, *C. rubrum*, and the red gorgonian, *P. clavata*, show a patchy distribution in the Western Mediterranean and neighboring Atlantic. They are gonochoric and longlived (tens of years) species displaying annual reproductive cycles, slow population dynamics (Linares et al. 2008; Torrents et al. 2005), and contrasting modes of reproduction. While *P. clavata* is a surface-brooder (Linares et al. 2008; Torrents and Garrabou 2011) and *C. rubrum* is an internal brooder, the two species produce lecithotrophic ciliated planulae. In aquaria, these larvae display similar median longevity, around 30 days, but contrasting swimming vs. non-swimming behaviors for *C. rubrum* and *P. clavata*, respectively (Guizien et al. 2020). They are impacted by various drivers of global change (Linares and Doak 2010), notably by warming-induced large-scale mass mortality events (MME; Garrabou et al. 2019). The population genetic structure of shallow populations has been characterized in the two species from local (Mokhtar-Jamaï et al. 2013; Ledoux et al. 2020) to regional (Ledoux et al. 2018; Gazulla et al. 2021) and global scales (Aurelle et al. 2011; Mokhtar-Jamaï et al. 2011). These studies demonstrated the occurrence of significant genetic differentiation among populations separated

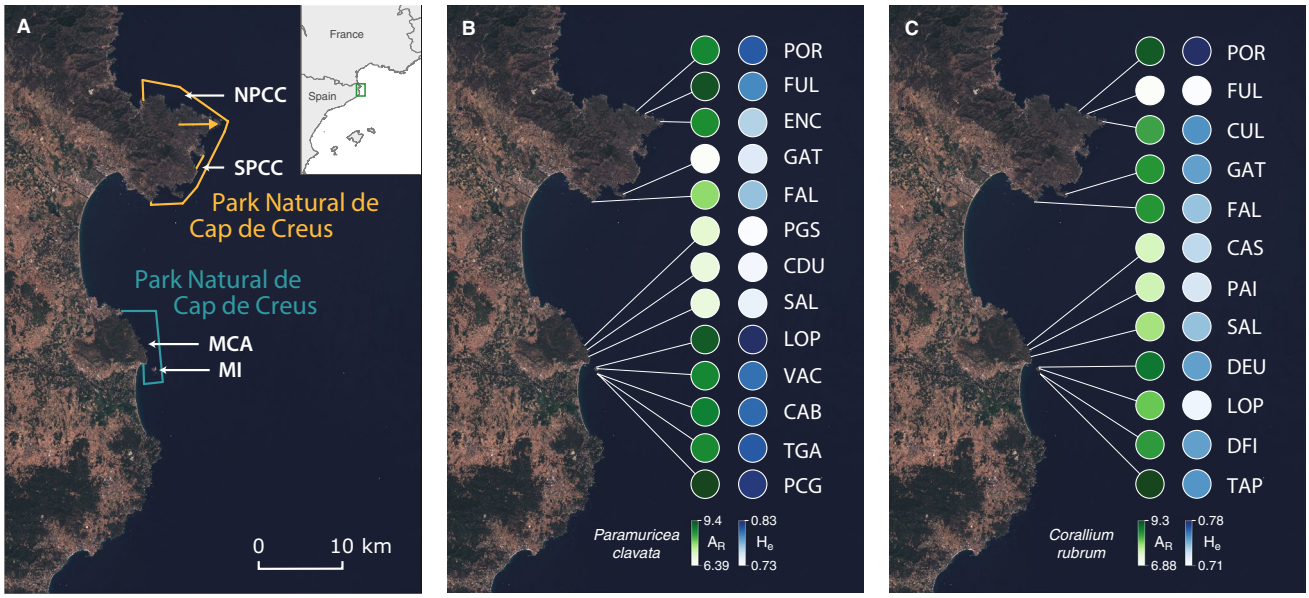

Fig. 1 The two Marine Protected Areas, "Park Natural de Cap de Creus" and "Park Natural del Montgrí, Medes Islands and Baix Ter" on the Catalan coast in the northwestern Mediterranean Sea. The white arrows specify the four areas (NPCC- northern part of Cap de Creus, SPCC- southern part of Cap de Creus, MCA- Montgri coastal area, MI- Medes islands). The yellow arrow delineates the Northern and Southern parts of Cap de Creus (panel A). The location of the 13 sampling sites of *Paramuricea clavata* (panel B) and of the 12 sampling sites of *Corallium rubrum* (panel C) is shown (see Table 1 for details). For each sampling site in each species, we show the rarefied allelic richness ($Ar_{(30)}$) and the gene diversity (H_e)

by tens of meters and complex spatial patterns combining genetic clusters and isolation by distance at both global and regional scales. Besides suggesting restricted gene flow among populations, these studies also supported the occurrence of shared genetic discontinuities in the two species at regional scale.

Sampling, DNA extraction, microsatellite genotyping, and genetic diversity analyses

The final dataset included 407 individuals from 13 sampling sites for *P. clavata* and 450 individuals from 12 sampling sites for *C. rubrum*, genotyped with seven and nine microsatellites, respectively (Table 1; Fig. 1). These two sets of markers were developed and used in previous genetic studies of the two species (e.g., Ledoux et al. 2010, Mokthar-Jamaï et al. 2011). To allow for the most rigorous comparison possible, both species were sampled at eleven shared or nearby (tens of meters) sites and, at each site, sampling was performed to cover the entire site. We provide specifics on sampling methods, DNA extraction, microsatellite genotyping, quality check, tests for linkage disequilibrium and departure from panmixia in Appendix A.

Computed estimates of genetic diversity include observed heterozygosity (H_o), gene diversity (H_e; Nei 1973), rarefied (Ar_g) and private allelic richness (Ap_g), and inbreeding coefficient (f estimator of F_{IS}; Weir and Cockerham 1984). We compared H_e and Ar_g for each species between the two MPAs using Wilcoxon signed rank tests.

We determined the statistical power of the two sets of microsatellites to detect genetic differentiation using POWSIM4.1 (Ryman & Palm 2006). We conducted simulations considering ten populations with effective size of 5,000 evolving during different numbers of generations (10, 20, 30, 40, 50, 100, 250, 500). These simulations resulted in eight levels of genetic differentiation among population-pairs estimated with Nei's (1987) estimator of pairwise F_{ST} (0.001, 0.002, 0.003, 0.004, 0.005, 0.01, 0.025, 0.047). Those simulated F_{ST} are within the range of the pairwise F_{ST} computed in each species (see Results). The power of each dataset to detect genetic structure for a given F_{ST} value was calculated by the proportion of significant Fisher's test per 1,000 replicates (see Appendix B).

Pattern of genetic structure

To explore the population genetic structure, we conducted a clustering analysis with STRUCTURE 2.2 (Pritchard et al. 2000) and a discriminant analysis of principal components (DAPC, Jombart et al. 2010) using ADEGENET (Jombart 2008), which are described in Appendix C.

In addition, we characterized the congruence of the spatial genetic patterns of *P. clavata* and *C. rubrum* using multiple factor analysis (MFA) focusing on the 11 sampling sites

Table 1 Characteristics of the samples

Species	MPA	Area	Location name	Name	Depth (m)	Latitude	Longitude	N
Corallium rubrum	Cap de Creus Natural Park	Northern Part of Cap de Creus (NPCC)	Portaló	POR	35–40	42.3331	3.2857	34
			Fullola	FUL	24	42.3302	3.2966	23
			Punta Culip	CUL	18	42.3252	3.3111	40
		Southern Part of Cap de Creus (SPCC)	El Gat Nord	GAT	30–35	42.2387	3.2655	45
			Punta Falconera	FAL	30–35	42.2325	3.2189	47
	Montgrí, Medes Islands and Baix Ter Natural Parc	Medes Islands (MI)	Pedra de Déu	DEU	45	42.0501	3.2248	30
			Potal del Llop	LOP	35	42.0497	3.2254	48
			Dofi	DFI	33	42.0439	3.2264	45
			Tascó Petit	TAP	40	42.0410	3.2270	41
		Montgrí Coastal Area (MCA)	Cap Castell	CAS	22	42.0815	3.2024	40
			Paieta	PAI	17–20	42.0641	3.2121	30
			Punta Salinas	SAL	20	42.0614	3.2142	35
Paramuricea clavata	Cap de Creus Natural Park	Northern Part of Cap de Creus (NPCC)	Portaló	POR	20–23	42.3331	3.2857	25
			Fullola	FUL	20	42.3302	3.2966	34
			L'Encalladora	ENC	18	42.3214	3.3212	30
		Southern Part of Cap de Creus (SPCC)	El Gat	GAT	20	42.2387	3.2655	32
			Punta Falconera	FAL	25	42.2325	3.2189	41
	Montgrí, medes islands and Baix Ter Natural Parc	Medes Islands (MI)	Carall Bernat	CAB	15	42.0422	3.2282	30
			Parcela Carall	PCG	15	42.0420	3.2279	30
			Pota del Llop	LOP	20	42.0497	3.2254	29
			Tascó Gran	TGA	15	42.0422	3.2269	30
			Vaca	VAC	23	42.0481	3.2263	38
		Montgrí Coastal Area (MCA)	Punta Salinas	SAL	22	42.0614	3.2142	37
			Cap d'Utrera	CDU	20–25	42.0689	3.2120	28
			Puig de la Sardina	PGS	20–25	42.0738	3.2083	28

common to both species (i.e., excluding DEU for *C. rubrum* and PCG and VAC for *P. clavata*). MFA is a canonical ordination method for summarizing and visualizing correlations among several matrices based on their individual PCAs. The contribution of all the matrices defines the distance between populations (Borcard et al. 2018). For each species, allele frequencies were scaled using scaleGen function in ADEGENET (Jombart 2008). A third matrix of latitude and longitude was included to account for the spatial location of each site. Correlations among the three matrices were described using RV coefficients, a multivariate generalization of the squared Pearson's correlation coefficients. The MFA among the three matrices and estimation of RV coefficients were conducted in the R package FACTOMINER (Le et al. 2008).

Secondly, for each sampling site, we calculated the population-specific F_{ST} and 95% High Probability Density Intervals in GESTE (Foll & Gaggiotti 2006) for each sampling site. This method measures the genetic differentiation proper to each sampling site and estimates the relative impact of genetic drift on the differentiation of the considered sampling site relative to the remaining ones.

Third, we looked for isolation by distance (IBD) patterns and estimated related demographic parameters. We used GENEPOP 4.1.4 (Rousset 2008) to compute the overall F_{ST} (Weir & Cockerham 1984) and the pairwise F_{ST} in each species. Because our quality check reveals the occurrence of null alleles in the two species (see Results), we compared the values obtained with GENEPOP with those obtained with the ENA method implemented in FreeNA (Chapuis & Estoup 2007), using a Mantel test with 10,000 permutations. Owing to the strong correlation among the two F_{ST} matrices (see Results), we considered the impact of null alleles to be limited and conducted the analyses using F_{ST} from GENEPOP. Genotypic differentiation between sampling sites was tested using an exact test (Raymond & Rousset 1995) with default parameters. In each species, the IBD was tested with a Mantel test in GENEPOP with 10,000 permutations to test the significance of the correlation between pairwise genetic ($F_{ST}/(1-F_{ST})$ and geographic distances ($ln(d)$) among pairs of sampling sites. The geographic distances were estimated considering the shortest path between sampling sites accounting for the topography (e.g. islands). We estimated the 'neighborhood size', a parameter function of

the effective dispersal and density, as the inverse of the slope of the linear regression (Rousset 1997).

Finally, we compared two estimators of genetic differentiation in each species: F_{ST} and D_{EST} (Jost 2008). These estimators provide complementary information about genetic patterns allowing to estimate the relative impact of fixation (F_{ST}) vs. allelic differentiation (D_{EST}) on the differentiation among sampling sites (Jost et al. 2018). We computed global and pairwise D_{EST}s in GENODIVE (Meirmans and vanTienderen, 2004). First, we compare the impact of allelic differentiation for each species by comparing their mean allelic differentiations (mean D_{EST} over all pairwise comparisons within a species) using a Welch Two Sample t-test. Then, we tested whether the strength of fixation differed among the two species. We thus tested for homogeneity of the regression slopes among pairwise F_{ST}s and D_{EST}s estimates looking at the interaction term in an ANCOVA framework (Andrade & Estévez-Pérez 2014). F_{ST} was modelled as the dependent variable with species as the factor and D_{EST}s as the covariate.

Individual-based assignment to sampling sites

Simulation study (Carlson 2008) demonstrated that assignment accuracy can reach 90% with F_{ST} as low as 0.05, which is close to the mean F_{ST} computed in our study for both species (see Results). Thus, for each species, we conducted a filtered assignment analysis following Lukoschek et al. (2016) to compare their relative patterns of demographic connectivity. This three-step analysis was conducted using GENECLASS2 (Piry et al. 2004). First, we identified first-generation migrants (FGMs) in each species using the Bayesian criteria of Rannala and Mountain (1997) with 10,000 simulated genotypes and an alpha of 0.01. Then, for each species considered separately, FGMs were removed from the dataset and re-assigned to the reference dataset (i.e. dataset without FGMs). As a third step, migrants were assigned to a sampling site if their assignment probability was > 0.1. We allowed for multiple assignments (i.e. one individual assigned to different sampling sites). A migrant was considered as coming from an unsampled sampling site when the assignment probability was lower than 0.1 for all sampling sites.

Effective population sizes and demographic histories

We inferred potential past changes in population size for each sampling site in each species using the model of a single population with a single discrete past variation in population size implemented in MIGRAINE (Leblois et al. 2014). The model considers a single panmictic population with an ancestral population size (N_{anc}) which suddenly decreased to its current population size (N) T_g generations ago, and infers three scaled parameters: the scaled ancestral population size ($\theta_{anc} = 2*N_{anc}*\mu$), the scaled current population size ($\theta_{cur} = 2*N*\mu$) and the scaled time at which the population size change occurred ($T = T_g*\mu$), with μ corresponding to the mutation rate. All population sizes are expressed as the number of genes. Those parameters are inferred from the data using the class of coalescent-based importance sampling algorithms (Iorio and Griffiths 2004a, b; Leblois et al. 2014) and accounting for a generalized stepwise-mutation model (*GSM*). MIGRAINE also infers *p*GSM the shape of the geometric distribution determining the size of stepwise microsatellite mutations in the GSM. The detection of past changes in population size is based on the ratio of population size ($N_{ratio} = N/N_{anc}$). A $N_{ratio} > 1$ corresponds to a population expansion and a $N_{ratio} < 1$ to a bottleneck / population contraction. In *C. rubrum*, the analyses were conducted excluding Mic27 due to the intricated mutation model (i.e. eight loci in total). For the sampling sites with stable population size (i.e. $N_{ratio} = 0$; see Results), we run the one-population model in MIGRAINE to estimate the current scaled population size ($\theta_{cur} = 2*N*\mu$). The numbers of trees, points and iterations are shown in Appendix D. Noteworthy, isolation by distance (IBD) can affect demographic inferences. Yet, the relatively weak IBD signal reported for the two species (neighborhood size > 100 individuals; see Results) combined to the large sampling scale for each sampling site (i.e., sampling over the whole area) limit the potential impact of IBD on demographic inferences (see Leblois et al. 2014).

For multiple tests, significance levels were corrected using a false discovery rate (FDR) correction (Benjamini and Hochberg 1995).

Results

Linkage disequilibrium. panmixia and genetic diversity

In *P. clavata*, significant linkage disequilibrium after false discovery rate correction was reported between *Pcla-14* and *Pcla-09* in CDU and between *Pcla-a* and *Pcla-10* in CSA. The mean frequencies of null alleles per sampling site were low, between 0.005 for TAG and 0.023 for ENC. Observed heterozygosity (H_o) values were between 0.71 for SAL and ENC and 0.83 for TGA (mean over sampling sites ± SE = 0.76 ± 0.04). The gene diversity (H_e) ranged between 0.73 (PGS and CDU) and 0.83 (LOP and PGC) (mean over sampling sites ± SE = 0.78 ± 0.04). The *f* estimator of F_{IS} varied between −0.02 (TGA) and 0.07 (ENC) (mean over sampling sites ± SE = 0.03 ± 0.03). No significant departure from panmixia was observed based on exact tests in any sampling site. The lowest and highest values of $Ar_{(30)}$

were observed for GAT (6.39) and PCG (9.40) (mean $Ar_{(30)}$ over sampling sites ± SE = 8.23 ± 1.06). The lowest and highest values of $Ap_{(30)}$ were observed for TGA (0.09) and FUL (0.51) (mean $Ap_{(30)}$ over sampling sites ± SE = 0.2 ± 0.12) (see Table A2; Fig. 1).

In *C. rubrum*, no significant linkage disequilibrium was observed. The mean frequencies of null alleles per sampling site were between 0.15 for CAS and 0.22 for FUL with a mean value over sampling sites = 0.18. Yet, estimates of genetic diversity are robust to such high frequencies of null alleles (see Chapuis et al. 2008). Observed heterozygosity values (H_o) were between 0.45 for GAT and 0.55 for TAP and DEU (mean over sampling sites ± SE = 0.52 ± 0.03). The gene diversity (H_e) ranged between 0.71 (FUL and LOP) and 0.78 (POR) (mean over sampling sites ± SE = 0.74 ± 0.02). The f estimator of F_{IS} varied between 0.27 (DEU, LOP, CAS) and 0.40 (GAT) (mean over sampling sites ± SE = 0.3 ± 0.04). The exact tests revealed significant departure from panmixia in all the sampling sites (after FDR correction). The lowest and highest values of $Ar_{(30)}$ were observed for FUL (6.88) and TAP (9.3) (mean $Ar_{(30)}$ over sampling sites ± SE = 8.36 ± 0.72). The lowest and highest values of $Ap_{(30)}$ were observed for LOP (0.17) and POR (0.86) (mean $Ap_{(30)}$ over sampling sites ± SE = 0.43 ± 0.22) (see Table A2; Fig. 1).

Regarding the comparisons between MPAs for a given species and among species, the Wilcoxon signed rank tests did not show any significant differences in the level of genetic diversity (H_e and $A_{r(g)}$).

Pattern of genetic structure

The simulations conducted in POWSIM supported the statistical power of our dataset to detect genetic structure corresponding to F_{ST} equals to 0.005 (see Appendix B). This value is one order of magnitude lower than the global F_{ST} computed for *P. clavata* (0.049) and *C. rubrum* (0.041).

In *P. clavata*, the Evanno's method (see Appendix C Figure C1) identified four different genetic clusters ($K = 4$; Fig. 2A). These four genetic clusters were concordant with

Table 2 MIGRAINE analyses conducted in the two species, *Corallium rubrum* and *Paramuricea clavata*

Species	Sample	Time of population change Tg*μ [95% CI]	Current population size 2N*μ[95% CI]	Ancestral population size $2N_{anc}$*μ [95% CI]	Nratio [95% CI]
Corallium rubrum	POR	3.9 [0.7–14.9]	5.9 [4.4–17.3]	1,164 [9.5–3902]	**0 [0–0.2]**
	FUL		3.1 [2.7–4.3]		0 [0–6.9]
	CUL	1.4 [0.5–5.2]	4.7 [3.3–6.5]	104.4 [15.7–14878]	**0 [0–0.3]**
	GAT	2.4 [0.1–656.2]	4.5 [3.4–5.8]	41,509 [4.9–128395]	**0 [0–1]**
	FAL	2.6 [0.7–5.6]	4.6 [3.4–6.2]	12,879 [11.9–NA]	**0 [0–0.4]**
	DEU		4.9 [3.6–6.7]		0 [0–177.5]
	LOP	3 [0.02–8.6]	4.7 [3.6–6.1]	17,438 [7.4–NA]	**0 [0–0.1]**
	DFI	3.1 [0.4–8.9]	4.9 [3.6–6.4]	2,404 [6.8–4560]	**0 [0–0.1]**
	TAP	1.6 [0.5–6.9]	6 [4.3–8.1]	61.7 [12.6–51496]	**0.1 [0–0.1]**
	CAS	2.2 [0.5–5.6]	3.7 [1.8–5]	1,506 [5.9–NA]	**0 [0–0.3]**
	PAI	2.4 [0.6–6.2]	3.5 [2.5–4.8]	18,465 [6.9–NA]	**0 [0–0.5]**
	SAL	1.1 [0.5–2.9]	4.5 [3.1–6.4]	83.4 [20–666.6]	**0.1 [0–0.2]**
Paramuricea clavata	POR		5.9 [4.2–8.58]		10.2 [0–12,581]
	FUL		6.8 [4.9–9.3]		0.7 [0–4,266]
	ENC		5.7 [4.1–7.8]		3.8 [0–5,060]
	GAT		2.9 [2–4.2]		0 [0–4,839]
	FAL		4.7 [3.4–6.5]		60.5 [0–350.3]
	CAB		6.4 [4.5–9]		1,142 [0–NA]
	PCG		8.8 [6.1–12.5]		691.2 [NA–1,382]
	LOP		6.8 [4.8–9.5]		16,151 [0–35,574]
	TGA		6.4 [4.5–9]		0 [0–24,901]
	VAC		6.1 [4.4–8.4]		0.1 [0–13,442]
	SAL	0.1 [0.1–4]	0.1 [0.1–2.8]	4.2 [2.8–23.4]	**0 [0–0.8]**
	CDU		3.5 [2.4–4.9]		0 [0–232.5]
	PGS		3.6 [2.5–5.1]		0 [NA–258.8]

Nratio values in bold are significantly lower than 1 corresponding to a population bottleneck (i.e. 95% CI excluding 1), while *Nratio* values not bold correspond to a stable population signal with 95% CIs including 1 (see main text for details)

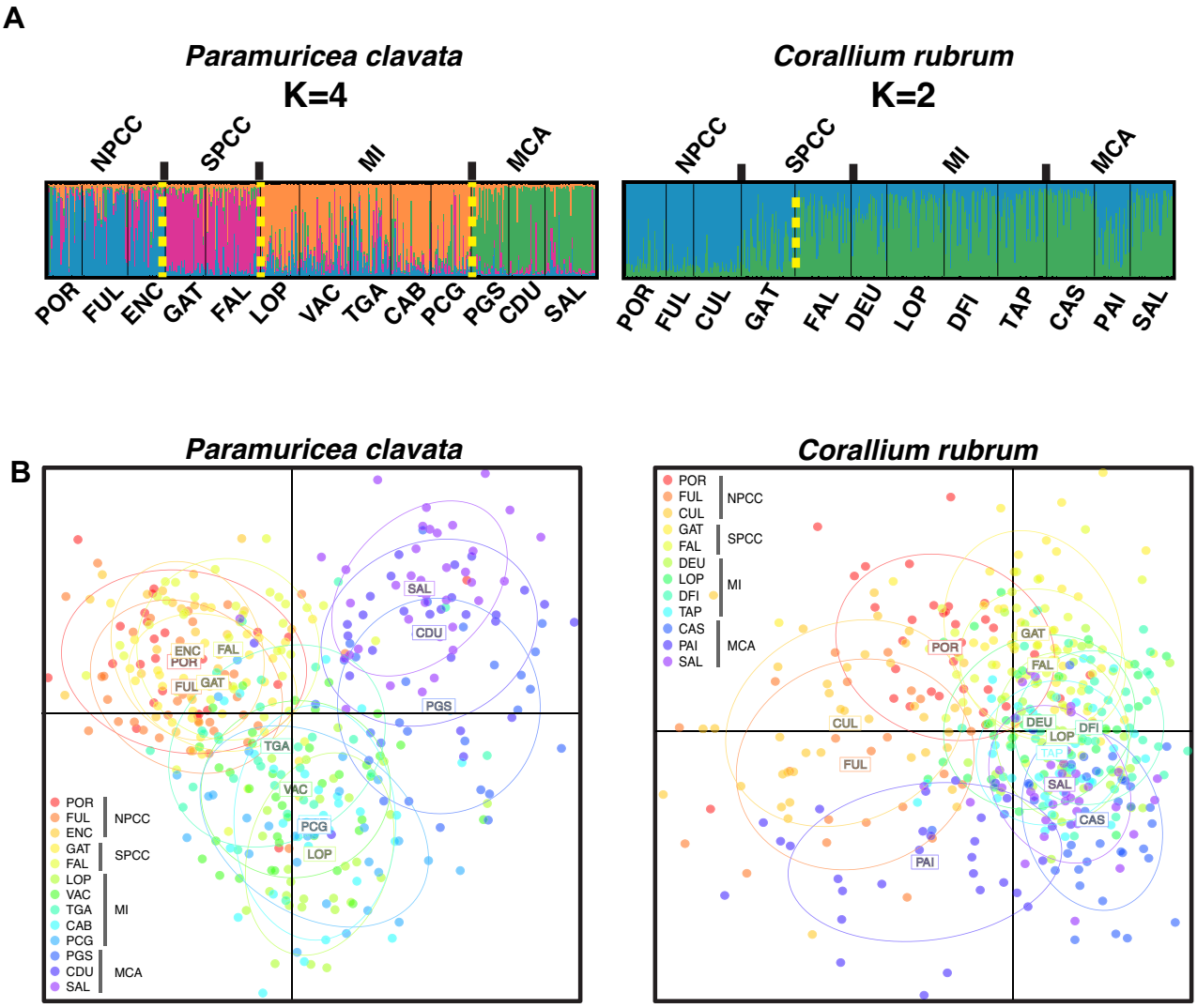

Fig. 2 Spatial genetic structure: **A** Clustering analysis conducted with STRUCTURE considering K = 4 for *Paramuricea clavata* (left panel) and K = 2 for *Corallium rubrum* (right panel). Each individual is represented by a vertical line partitioned in *K*-colored segments, which represent the individual membership fraction to *K* clusters. Thin and thick black vertical lines delineate the different locations and regions, respectively. Sample names (see Table 1) and areas (NPCC: northern part of Cap de Creus, SPCC: southern part of Cap de Creus, MI: Medes Islands, MCA: Montgrí coastal area) are shown below and above the assignment plots. Thick yellow doted lines delineate main genetic discontinuities. **B** Scatter plots of the discriminant analysis of principal components (DAPC). Each dot corresponds to one individual from each sampling site, which are represented by different colors. Inertia ellipses centre on the mean for each location and include 67% of the sampling points. The area of origin of each sample sites is shown in the two plot legends (see Table 1 for details)

the areas corresponding to the northern part of Cap de Creus (NPCC, mean membership coefficient = 0.69) and the southern part of Cap de Creus (SPCC, mean membership coefficient = 0.73), the Medes Islands (MI, mean membership coefficient = 0.63) and Montgrí (MCA, mean membership coefficient = 0.78).

In *C. rubrum*, the Evanno's method (see Appendix C Figure C1) identified two different genetic clusters ($K = 2$) that encompassed the individuals from the northern part of Cap de Creus (NPCC) and GAT (mean membership coefficient = 0.81) vs. the remaining individuals (mean membership coefficient = 0.69), except individuals from PAI, which were almost equally shared between the two clusters.

The DAPC analyses corroborated these results. The first two axes represented similar levels of the total variation in the two datasets (47.8% and 49.3% in *P. clavata* and *C. rubrum*, respectively). The scatter plot is more concordant with a geographic imprint in *P. clavata* compared to *C. rubrum* (Fig. 2B). The first axis segregated *P. clavata* individuals from Cap de Creus (NPCC + SPCC)

and Montgrí (MCA) with an intermediate position for Medes Islands (MI). The second axis divided Cap de Creus (NPCC + SPCC) and Montgrí (MCA) from Medes (MI) sampling sites. In *C. rubrum*, individuals from CUL/FUL (Cap de Creus) were separated from the remaining ones along the first axis with an intermediate position for POR (Cap de Creus) and PAI (Montgrí). Individuals from PAI (Montgrí) and POR/GAT (Cap de Creus) were scattered at the two extremes of the second axis with all the Medes individuals in an intermediate position.

Overall, the two analyses supported a stronger geographic imprint in *P. clavata* compared to *C. rubrum*. The STRUCTURE analyses also revealed a different genetic discontinuity in the two species: Montgri (MCA) vs. remaining individuals in *P. clavata* and northern part of Cap de Creus (NPCC) vs. remaining individuals in *C. rubrum* (Fig. 2).

The MFA showed a global congruence in the spatial patterns of genetic variation between *P. clavata* and *C. rubrum*. Allele frequencies across sites were significantly correlated between the two studied species (RV coefficient = 0.74, p-value = 0.013). This positive correlation and the similar strength and direction of the groups of variables "allele frequencies" for *C. rubrum* and *P. clavata* confirmed a positive correlation between those two groups (Fig. 3 inset (ii)). This positive correlation was also true (but lower) between the groups of variables "alleles frequencies" and "latitudes/longitudes" (Fig. 3 inset (ii)). The two species showed a significant but moderate correlation between allele frequencies and spatial location (*C. rubrum*: RV = 0.51, p-value = 0.012; *P. clavata*: RV = 0.56, p-value = 0.004). The first dimension of the MFA differentiated northern from southern sites (i.e. the two MPAs) explaining 34.7% of the total variance. The second dimension (16.7% of the total variance) showed a relatively strong genetic differentiation between Medes Islands and Montgrí for *P. clavata* (blue dots in Fig. 3) despite short geographic distances (green dots in Fig. 3).

In *P. clavata*, the lowest population-specific F_{ST} was observed for PCG (Medes Island; 0.020 95% CI: 0.001–0.032) whereas GAT (southern Part of Cap de Creus) showed the highest value (0.105 95% CI: 0.069–0.146). Based on 95% CI, Medes Islands sampling sites showed significantly lower values than Montgrí sampling sites. In *C. rubrum*, the population-specific F_{ST}s ranged between 0.044 (95% CI: 0.031–0.057) for TAP (Medes Islands) and 0.122 (95% CI: 0.086–0.156) for FUL (northern Part of Cap de Creus). The lowest population-specific F_{ST}s were observed for Medes Islands sampling sites. Except for FUL from the Northern Part of Cap de Creus, the population-specific F_{ST}s in *C. rubrum* were more homogeneous compared to *P. clavata* with

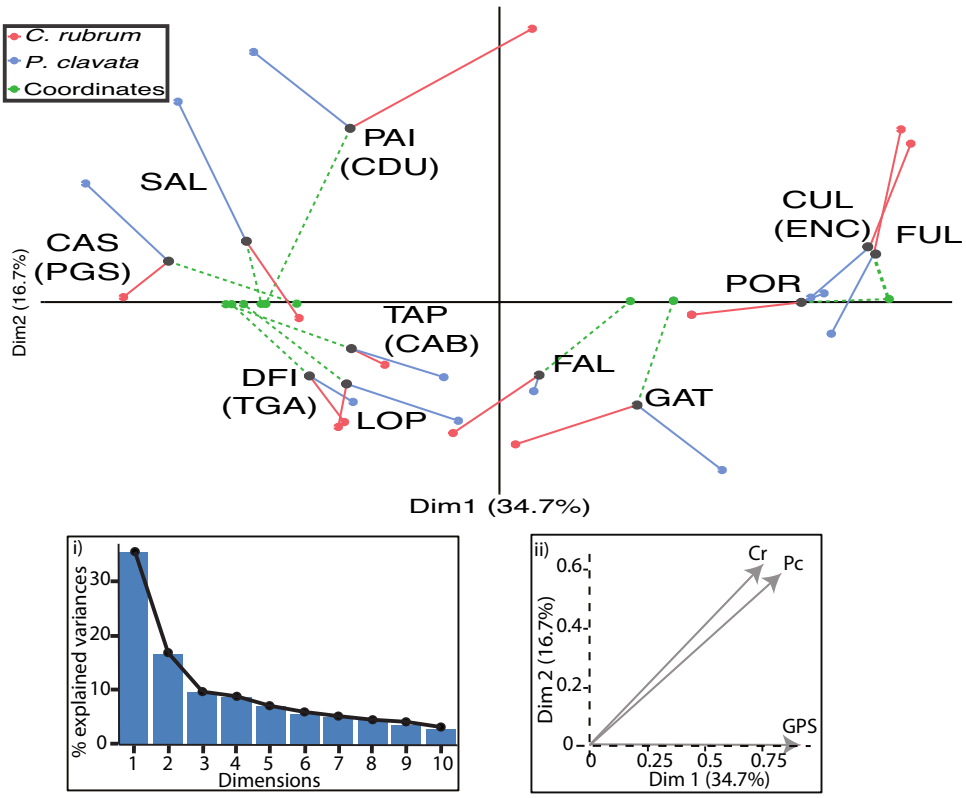

Fig. 3 Multiple Factorial Analysis (MFA) accounting for the matrices of allele frequencies in *P. clavata* (blue) and *C. rubrum* (red) and spatial coordinates (latitude and longitude; green). The grey dots correspond to the MFA centroids. Sampling site names are shown as in Table 1, with the sampling sites from *P. clavata* dataset between parentheses. Inset (i) shows the percentage of explained variation function of the number of axes. The first 2 axes explained 51.4% of the total variance. Inset (ii) shows the correlation among the three matrices (allele frequencies in the two species and spatial coordinates) along the first two axes

an overlap for most of the 95% CI including those from Montgrí sampling sites (Appendix A, Fig. 4A).

In *P. clavata*, the exact tests for genotypic differentiation were significant at the global level and 72 pairwise comparisons (92%; see Appendix E). The six non-significant tests involved pairs of close-by sampling sites from Medes Islands separated by 36 to 870 m. The pairwise F_{ST} values ranged from $2*10^{-4}$ for LOP *vs.* PCG and 0.141 for GAT *vs.* PGS. The correlation among the genetic (F_{ST}/(1-F_{ST})) and the geographic distance (*ln(d)*) was significant suggesting a pattern of IBD among the 13 sampling sites (p-value = 0.02; Fig. 4B). The slope of the regression was 0.0078 [95% CI: 0.0054; 0.0101] resulting in a neighborhood size *Nb* equals to 128 [95% CI: 99; 185] individuals.

In *C. rubrum*, the exact tests for genotypic differentiation were significant at the global level and for all the pairwise comparisons, even when considering DEU *vs.* LOP separated by only 79 m (see Appendix E). The pairwise F_{ST}s ranged from 0.01 for FUL *vs.* CUL and 0.10 for CAS *vs.* FUL. The genetic distance (F_{ST}/(1-F_{ST})) and the geographic distance (*ln(d)*) were significantly correlated suggesting a pattern of IBD among the 12 sampling sites (p-value = 0.03; Fig. 4B). The slope of the regression was 0.005 [95% CI: 0.0032–0.0081] resulting in a *Nb* equals to 200 [95% CI: 124–313] individuals.

The Welch t-test supported a significant difference between the mean pairwise D_{EST} for *C. rubum* (0.13) and the mean pairwise D_{EST} for *P. clavata* (0.18) (p-value = $6.8*10^{-5}$). The study of the homogeneity of the regression slopes revealed that the interaction (D_{EST} * species) was significant (p-value = 0.002). Accordingly, the slopes of the two regression lines (0.328 for *C. rubrum* vs. 0.298 for *P. clavata*) are significantly different, suggesting differences in the rate of change of pairwise F_{ST}s function of D_{EST}s. For the same D_{EST}, *C. rubrum* has a higher F_{ST} than *P. clavata* (Fig. 4C).

The pattern of connectivity among sampling sites

In *P. clavata*, 12 of the 407 individuals (3%) were considered first-generation migrants (FGMs). PCG and LOP (Medes Islands, MI) were identified as the main sources of FGMs. One FGM was identified in ENC, FAL, TGA, VAC, SAL, CDU and PGS, and two and three were identified CAB and GAT, respectively. Four sampling sites (POR, FUL, PCG, LOP) did not show any FGM. Considering assignment probability > 0.1 and allowing for multiple assignments, we successfully assigned eight FGMs (67%) to seven sampling sites suggesting that one-third of the FGMs came from unsampled sampling sites. No migrants were produced by six sampling sites, including the two sampling sites from the southern part of Cap de Creus (SPCC) and the three sampling sites from Montgrí (MCA).

In *C. rubrum*, 18 of the 450 individuals (4%) were considered FGMs. CUL, TAP and SAL did not show any FGM while one (e.g. FUL) to three (e.g. POR) FGMs were identified in the remaining sampling sites. Only six (34%) FGMs were successfully assigned indicating that most of the FGMs came from unsampled sampling sites. TAP (Medes Islands, MI) was identified as the primary source of FGMs, while none of the migrant were produced by seven sampling sites (two from the southern Cap de Creus [SPCC] and two from Montgrí [MCA]).

Demographic histories and effective population size

In *P.clavata*, only SAL showed demographic contraction (*Nratio* < 1) characterized by a $T_g\mu$ (the product of the time of occurrence in generation with the mutation rate), a θ_{cur} (the current scaled population size) and a θ_{anc} (the ancestral scaled population size) equal to $2*10^{-6}$ (95% CI: $6*10^{-7}$–4,037), 0.1 (95% CI: 0.1–4) and 4.2 (95% CI: 2.8–23.4), respectively. The lack of mutation rate (μ) for microsatellites in octocorals precludes accurate estimations of the unscaled parameters. Yet, a first approximation can be obtained considering $\mu = 5*10^{-4}$ estimated in humans (Sun et al. 2012). In this case, the contraction occurred 0.004 (95% CI: 0.0012–8,940) generations ago (T_g), with *N* equal to 1 individual (95% CI: 1–1,414) and N_{anc} equal to 2,103 individuals (95% CI: 1,383–11,720). All the remaining sampling sites showed demographic stability with *Nratio* values encompassing both > 1 and < 1. The effective population sizes (θ) for these demographically stable sites estimated with the one-population model in MIGRAINE range from 2.9 (95% CI: 2–4.2) for GAT to 8.8 (6.1–12.8) for PCG. This corresponds to *N* ranging from 1,458 individuals (95% CI: 1,000–2,084) for GAT to 4,415 individuals (3,061–6,290) for PCG (Appendix D; Table 2).

In contrast, in *C. rubrum*, all but two sampling sites (FUL and DEU) showed significant past demographic contraction (*Nratio* < 1) with $T_g\mu$ ranging between 1.1 (95% CI: 0.5–2.9) for SAL and 3.9 (95% CI: 0.7–14.9) for POR. These demographic contractions occurred between 2,222 (95% CI: 1,000–5,800) and 7,800 (95% CI: 1,400–29,800) generations ago for SAL and POR, respectively. The θ_{cur} are also relatively homogeneous ranging from 3.1 (95% CI: 2.1–14.5) for FUL to 6 (4.3–8.1) for TAP, which corresponds to 6,200 (95% CI: 4,200–29,000) and 12,000 (8,600–16,200) individuals, respectively. Except for SAL (θ_{anc} = 83.4 [95% CI: 20–666.6]), θ_{anc} showed a plateau with a high likelihood ratio for θ_{anc} higher than 20 to 30. While these plateaus limit the estimations of related point estimates and 95% CI estimations, they point toward high ancestral effective population sizes with values higher than N_{anc} 10,000 to 15,000 individuals (Appendix D; Table 2).

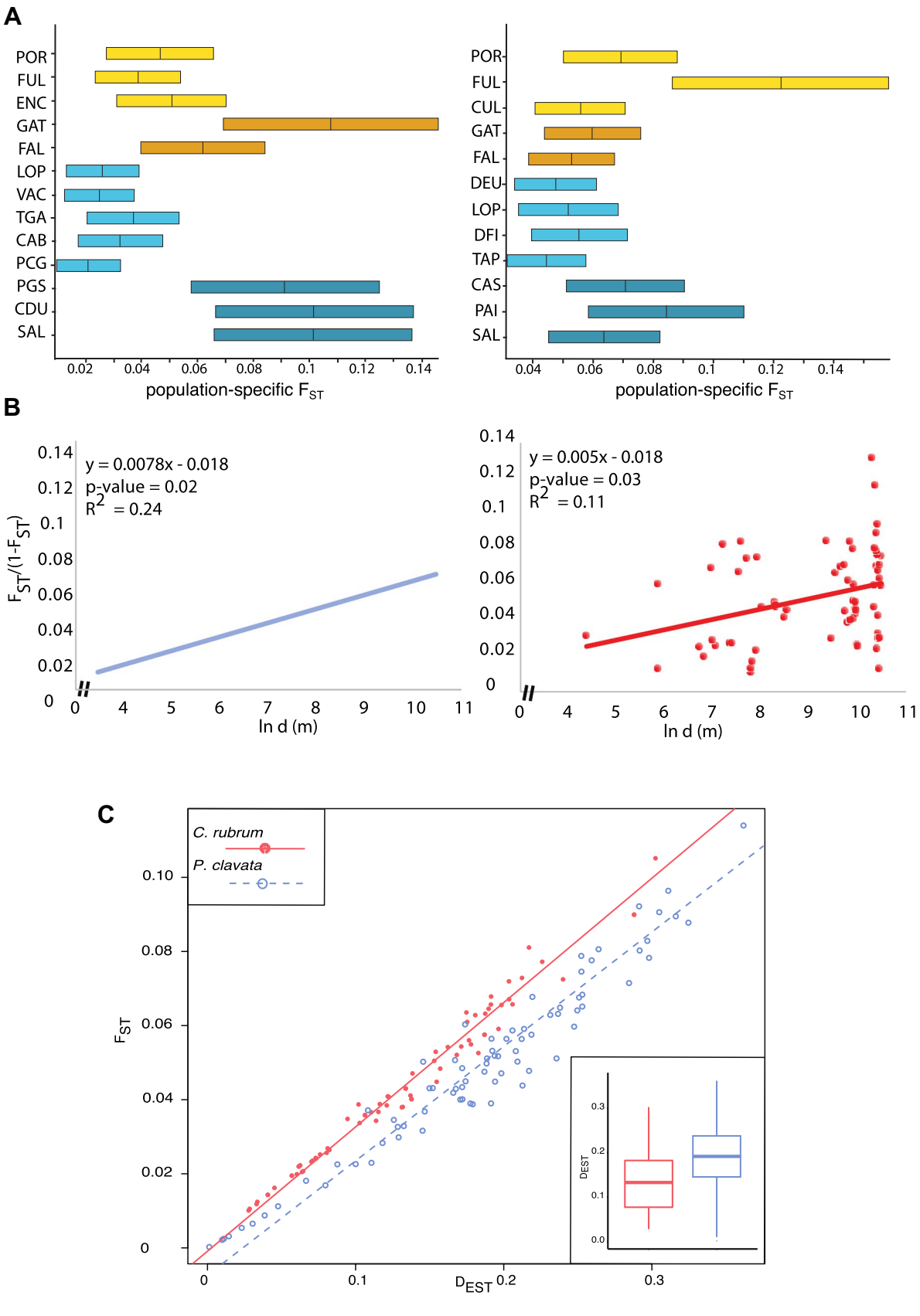
A
POR
FUL
ENC
GAT
FAL
LOP
VAC
TGA
CAB
PCG
PGS
CDU
SAL
0.02 0.04 0.06 0.08 0.1 0.12 0.14
population-specific F_{ST}
POR
FUL
CUL
GAT
FAL
DEU
LOP
DFI
TAP
CAS
PAI
SAL
0.04 0.06 0.08 0.1 0.12 0.14
population-specific F_{ST}
B
$F_{ST}/(1-F_{ST})$
y = 0.0078x - 0.018
p-value = 0.02
R^2 = 0.24
ln d (m)
y = 0.005x - 0.018
p-value = 0.03
R^2 = 0.11
ln d (m)
C
C. rubrum
P. clavata
F_{ST}
D_{EST}
DEST

◂**Fig. 4** **A** Population-specific F_{ST} for *P. clavata* (left panel) and *C. rubrum* (right panel). Each bar corresponds to the 95% highest posterior density interval while the mean value is show with a black line. The light and dark yellow bars correspond to the sampling sites from the Northern and Southern Part of Cap de Creus, respectively. The light and dark blue bars correspond to the sampling sites from Medes and Mongri, respectively. All values are shown in Appendix A. **B** Isolation by distance among populations in *P. clavata* (left panel) and *C. rubrum* (right panel). In the two species, the genetic distance (F_{ST}/(1-F_{ST})) among populations is significantly correlated with the geographic distance (ln(d) in m). **C** Linear regression among pairwise F_{ST}s (nearness to fixation) and D_{EST}s (Jost 2008; allelic differentiation) considering population pairs in *P. clavata* (blue) and *C. rubrum* (red). The regression slopes are significantly different between the two species, suggesting that for the same pairwise D_{EST}, the corresponding F_{ST} is higher in *C. rubrum* compared to *P. clavata*. Inset boxplot shows the mean D_{EST} values for each species (p value < 0.001)

Discussion

At a regional scale, previous studies suggested that the genetic patterns in *P. clavata* and *C. rubrum* are under similar influences of three main components: the origin of the samples, the occurrence of physical barriers to gene flow and the geographic distances among sampling site (e.g., Aurelle et al. 2011; Cahill et al. 2017). While we formally confirmed that the spatial genetic patterns are correlated in the two species (MFA, RV coefficient = 0.74), we built upon the comparative approach to reveal the contrasting impact of these three components. Linking these contrasts to a differential effect of genetic drift, we discuss the implications of our results for managing of the two species in the two MPAs.

Setting the scene: roughly similar but thoroughly different imprints of geography in the two species

We demonstrated a stronger influence of the origin of the samples on the genetic pattern in *P. clavata* compared to *C. rubrum.* Indeed, in *P. clavata*, the four clusters (mean membership coefficient 0.71) fit the four areas (Medes Islands, Montgrí Coastal Area, northern and southern parts of Cap de Creus). By contrast, only two diffuse clusters were observed in *C. rubrum* separating the northern part of Cap de Creus from the remaining sampling sites (mean membership coefficient 0.54). This first contrast between the two species is supported by the slightly higher correlation between allele frequencies and coordinates in *P. clavata* compared to *C. rubrum* (RV coefficients = 0.56 vs. 0.51).

The second contrast relies on the impact of potential physical barriers to gene flow. Indeed, the four clusters delineated in *P. clavata* suggested at least three main genetic discontinuities: northern vs. southern parts of Cap de Creus, Cap de Creus vs. Medes Islands/Montgrí coastal area and Medes Islands vs. Montgrí coastal area. In *C. rubrum*, the clustering analyses supported only one primary discontinuity between the northern part of Cap de Creus and the remaining sampling sites. A formal characterization of these barriers would require dispersal modelling through Lagrangian simulations (e.g. Reynes et al. 2021). It is however noteworthy that the only barrier shared between the two species is separating the northern and southern parts of Cap de Creus, which is in line with the highly contrasting oceanological conditions in these areas. The northern part of Cap de Creus is indeed submitted to more substantial and recurrent northern winds and near bottom current than the southern part (Gori et al. 2011).

The third difference observed between the two species was in the isolation by distance (IBD) pattern, with a stronger imprint of the geographic distance between sampling sites for *P. clavata* than for *C. rubrum* (R^2: 0.24 *vs.* 0.11). The lower fit of the correlation in *C. rubrum* is mainly driven by the high genetic distance existing among close populations from the same area (e.g. PAI vs. SAL in Montgrí). While the 95% CI interval overlapped, the trend toward a higher regression slope observed in *P. clavata* compared to *C. rubrum* induced the former to be characterized by a smaller neighborhood size. This result suggests a differential impact of the two components of the neighborhood size, the effective dispersal and the effective population density (Rousset 1997). However, this differential impact came opposite to the expectations based on characterizations of spatial genetic structure among individuals in *P. clavata* and *C. rubrum.* Previous studies indeed revealed a higher effective dispersal in the former [at a scale of a few meters in *P. clavata*; Mokthar Jamai et al. (2013) vs. at a scale of a few centimeters in *C. rubrum*; Ledoux et al. (2021)]. To solve this apparent paradox, one should account for the pairwise genetic differentiations involving sampling sites from Montgrí in *P. clavata*, which are inflated compared to the expectations from the IBD model.

Previous population genetics studies conducted in *C. rubrum* and *P. clavata* identified restricted gene flow among sampling sites rather than genetic drift as the leading force underlying the spatial genetic patterns. Restricted gene flow and connectivity among populations are likely the sources of the gross similar geographic imprint in the two species. Yet, the slight differences in gene flow and connectivity among the two species (e.g. almost similar estimates of neighborhood sizes) fall short of explaining the contrasting impacts of the sample origins, the barriers to gene flow and the geographic distances among samples previously discussed. We discuss below how genetic drift is thus likely to be the prominent driver of these differences.

The impact of genetic drift on population genetic structure in Mediterranean octocorals

The trend toward a higher mean population-specific F_{ST} in *C. rubrum* compared to *P. clavata* (0.064 vs. 0.056) supports a

stronger effect of genetic drift in *C. rubrum*. The steeper linear regression observed among the pairwise D_{EST} (allelic differentiation; Jost et al. 2018) and F_{ST} (nearness to fixation; Jost et al. 2018) in *C. rubrum* compared to *P. clavata* refines this result. The corresponding nearness to fixation estimate is higher in *C. rubrum* despite similar allelic differentiation. Noteworthy, the demographic histories of the two species are highly contrasted. While we cannot rule out a potential bias due to the lower number of microsatellites in *P.clavata* compared to *C. rubrum*, all *P. clavata* sampling sites, except SAL in Montgrí, displayed demographic stability. Yet, 80% of the red coral sampling sites (all but FUL and DEU) were impacted by demographic contractions occurring in a relatively recent past, as supported by the lower limit of the 95% CI of the scaled time of population change (T_g*μ) ranging between 0.02 for LOP and 0.7 for POR. These values correspond to unscaled times of population change ranging between 40 and 1,400 generations for LOP and POR, respectively. Demographic stability in *P. clavata* was already observed in populations from the Adriatic Sea (Ledoux et al. 2018). In spite of their contrasting demographic histories, the two species showed relatively similar current scaled population size (θ_{cur}), which can be approximate to a few thousand individuals (unscaled effective population sizes from 1 to 4,415 in *P. clavata* and from 1,535 to 2,988 in *C. rubrum*). Interestingly, almost all the lowest values in the two species are observed in the sampling sites from Montgri, supporting the particular features of this area. In the remaining sites, while the 95% CI are overlapping, our data suggests a trend toward slightly lower current scaled population sizes and, accordingly, higher genetic drift in *C. rubrum* compared to *P. clavata.* The unscaled effective population sizes and times of population change discussed here were computed considering the microsatellite mutation rate in humans ($\mu = 5*10^{-4}$; Sun et al. 2012). To refine these estimations, the microsatellite mutation rate in octocorals is needed.

Genetic drift is usually underrated in marine species owing to their assumed large effective population size (Riquet et al. 2016). However, many studies focused on effective population size had been done on long-dispersers, such as bentho-pelagic invertebrates displaying long larval phases, which is not a property of our study species. Our results, combined with previous studies (e.g., Crisci et al. 2017; Masmoudi et al. 2016), strengthened the need to reconsider the role of this evolutionary process in low-dispersive habitat-forming species, such as in the Mediterranean octocorals.

How to explain the differential impact of genetic drift in the two species?

Linking the differential impact of evolutionary drivers (e.g., gene flow, genetic drift) to ecological features and biotic or abiotic factors is challenging (Selkoe and Toonen 2011). Here, we assume a relatively low differential influence of abiotic factors because the two species have been sampled in proximate or common localities. Yet, because *P. clavata* is usually found in more open habitats than *C. rubrum*, the influence of local conditions cannot be ruled out to explain the lowest genetic isolation globally observed in the former. Regarding the biotic factors, these two long-lived species display relatively similar life history traits (Gómez-Gras et al. 2021). The larval longevity estimated in aquaria was similar in the two species (Guizien et al. 2020), in line with the comparable impact of gene flow previously discussed. The two species mainly diverged based on their reproductive strategy and contrasted fecundity (Linares et al. 2008; Torrents and Garrabou 2011). *C. rubrum* is an internal brooder with internal fertilization whereas *P. clavata* is a surface brooder with external fertilization. Moreover, the reproduction period is highly restricted in *P. clavata* (two events at the end of June; Linares et al. 2008) compared to *C. rubrum*, which is more diffuse (weeks to months during summer; Torrents and Garrabou 2011). These two traits can differentially influence the two species' reproductive success and genetic drift. Paternity analyses based on standardized protocols in the two species are required to investigate further this hypothesis. For instance, a hypothesis to be tested is whether the same total number of larvae from the same number of mothers in populations with comparable demographic characteristics is coming from the same number of fathers.

Human exploitation is another factor that could explain an increased genetic drift in *C. rubrum* compared to *P.clavata*. Indeed, the red coral is a precious octocoral harvested since Antiquity for its use in jewelry (Bruckner 2010). This pressure led to a shift in population demographic structure with subsequent impacts on its reproduction (Linares et al. 2010). Considering the establishment date of the MPAs (between 1983 and 2010) and the generation time of *C. rubrum* (sexual maturity at 10 years of age (Torrents and Garrabou 2011)), some of the demographic contractions revealed (e.g., in LOP) can be related to the harvesting records in this region (Tsounis et al. 2010). Yet, a formal link between the harvesting pressure and the demographic results is not straightforward. Firstly, the confidence intervals of $T_g\mu$ are relatively wide likely due to the limited number of genetic markers used in the study. Secondly, the method implemented in MIGRAINE has a limiting power to detect recent demographic event (Leblois et al. 2014).

Conservation implications: four management units with contrasting genetic characteristics

The contrasting patterns of genetic structure and the differential impact of genetic drift provide complementary insights that may support site prioritization in the two MPAs.

The genetic patterns did not overlap with any of the current MPAs' boundaries, even when considering intermediate clustering results for K = 2 in STRUCTURE. Instead, the pattern of genetic structure in *P. clavata* supports the definition of four distinct management units corresponding to four areas fitting with the spatial distribution of the four genetic clusters identified (northern and southern parts of Cap de Creus, Montgrí coastal area and Medes Islands). Noteworthy, these units are relatively poorly connected. For instance, in *P. clavata*, the mean memberships were 0.63 and 0.78 in Medes and Montgrí, respectively. These values are high considering the low distance between the two areas (< 2 km) and support the occurrence of differentiated gene pools. While the two MPAs can be considered as relatively independent on a contemporary time scale, some interactions exist and should be preserved, as supported by the intermediate STRU CTURE results (not shown), in which populations from the two MPAs are grouped in the same cluster (e.g., for K = 2 in *P. clavata* sampling sites from the southern part of the Cap de Creus and sampling sites from Medes Islands).

The genetic diversity of the two species is high and similar between the two species and between the two MPAs. It falls within the range of values previously reported in this region (Mokthar Jamai et al. 2011; Perez-Portela et al. 2016). The lower values of global F_{ST}s compared to D_{EST}s suggested heterogeneous distributions of the genetic diversities (see Jost et al. 2018). These patterns lead to the definition of hot- and a coldspots of genetic diversity, which are shared by the two species and correspond to the Medes and Montgrí management units, respectively. The Medes hotspot encompasses the main sources of first-generation migrants in the two species (PCG and LOP in *P. clavata* and TAP in *C. rubrum*) and is characterized by the lowest levels of genetic isolation, thus an important area for the connectivity network. The importance of this management unit for the connectivity of the system should help to reconsider the pressure resulting from the recreational diving in this part of the MPA (Linares et al. 2010). Although for opposite reasons, the conservation status of the coldspot of Montgrí, is also of concern. In this area, the populations of the two species are genetically depleted and isolated with the lowest current effective population sizes. Active restoration actions (e.g. Gazulla et al. 2021) should be considered to buffer the impact of genetic drift and putative related adverse effects such as inbreeding depression (Garner et al. 2020). Interestingly, these hot- and coldspots of genetic diversity correspond to the area protected since the longest (1983; almost 50 years) and the shortest (2010; 11 years) period. While caution is needed here, this observation suggests that conservation efforts are also effective in protecting biodiversity at the infra-species level, i.e. genetic diversity, which is required for the genetic adaptation of species to changing environments. It is also noteworthy that the only division shared between *C. rubrum* and *P. clavata* was reported between the northern vs. southern parts of Cap de Creus. The singularity of the genetic pools of the northern part of Cap de Creus has been previously reported in the fucoid algae *Treptacantha elegans* (Medrano et al. 2020), but not in the white gorgonian *Eunicella singularis* (Costantini et al. 2016).

Conclusion

The comparative approach developed here revealed that genetic drift is a critical although still underrated process to examine in long-lived and low dispersive Mediterranean octocorals. *C. rubrum* and *P. clavata* are habitat-forming species with key ecological role of in coralligenous community, one of the most diverse and most threatened Mediterranean communities. Accordingly, the management inputs previously discussed, including the necessity to reduce diving pressure on the Medes area, should benefit the whole coralligenous community. These recommendations based on neutral genetic diversity should be complemented. The pressure from the recurrent mass mortality events linked to ongoing warming raises the question of the future of these marine communities owing to the dramatic demographic declines observed in many species (Garrabou et al. 2019, 2021). In this context, characterizing the adaptive genetic diversity and more particularly potential genomic factors and processes driving the response to thermal stress is urgently needed to pave the way for effective management plans in the context of climate change.

Supplementary Information The online version contains supplementary material available at https://doi.org/10.1007/s10592-023-01573-8.

Acknowledgements Field work and sampling were done in accordance with legislations. Part of this work was carried out by using the resources of the national INRAe MIGALE (http://migale.jouy.inra.fr, MIGALE, INRAE, 2020. Migale bioinformatics Facility, https://doi.org/10.15454/1.5572390655343293E12) and GENOTOUL (Toulouse Midi-Pyrénées) bioinformatics HPC platforms, as well as the local Montpellier Bioinformatics Biodiversity (MBB, supported by the LabEx CeMEB ANR-10-LABX-04-01) and CBGP HPC platform services. This is publication ISEM 2023-192. JBL, DGG, PLS, CL and JG are part of the Marine Conservation research group MEDRECOVER (2017 SGR 1521) from the Generalitat de Catalunya.

Authors contribution JBL, CL and JG conceived the study. JBL, CL and JG collected the samples. JBL, PLS, RAM and EN performed the DNA laboratory work. JBL, MH, SD and RL analyzed the genetic data. FV contributed to data interpretation and analyses choices. MH and JBL wrote the paper with inputs from all co-authors.

Funding Open access funding provided by FCT|FCCN (b-on). JBL was funded by assistant researcher 2021.00855.CEECIND through national funds provided by FCT—Fundação para a Ciência e a Tecnologia. This research was supported by national funds through FCT within the scope of UIDB/04423/2020 and UIDP/04423/2020, by the MIMOSA

project funded by the Foundation Prince Albert II Monaco. This work was supported by the European Union's Horizon 2020 research and innovation program under grant agreement SEP-210597628 (FutureMARES). This study was also supported by the Spanish Government through the Smart project (CGL2012-32194) the HEATMED project (RTI2018-095346-B-I00, MCIU/AEI/FEDER, UE). RL was supported by the Agence Nationale de la Recherche (projects DISLAND ANR-20-CE32-00XXX, GENOSPACE ANR-16-CE02-0008 and INTROSPEC ANR-19-CE02-0011; and project PROLAG from the CeMEB LabEx;), and by recurrent funding from INRAe and CNRS. This research has been funded from the European Union's Horizon 2020 research and innovation programme under grant agreement No 869300 "FutureMARES". SD is supported by the*Fonds National de la Recherche Scientifique(FNRS, Belgium). JG and PL acknowledge the funding of the Spanish government through the 'Severo Ochoa Centre of Excellence' accreditation (CEX2019-000928-S). CL gratefully acknowledges the financial support by ICREA under the ICREA Academia program.*

Data availability Microsatellite genotypes will be available upon publication of the paper.

Declarations

Competing interests The authors declare no competing interests.

Conflict of interest We have no conflict of interest to declare.

References

Álvarez-Romero JG, Munguía-Vega A, Beger M, Mar Mancha-Cisneros M, Suárez-Castillo AN, Gurney GG et al (2018) Designing connected marine reserves in the face of global warming. Glob Chang Biol 24:e671–e691. https://doi.org/10.1111/gcb.13989

Andrade JM, Estévez-Pérez MG (2014) Statistical comparison of the slopes of two regression lines: a tutorial. Anal Chim Acta 838:1–12. https://doi.org/10.1016/j.aca.2014.04.057

Aurelle D, Ledoux J-B, Rocher C, Borsa P, Chenuil A, Féral J-P (2011) Phylogeography of the red coral (*Corallium rubrum*): inferences on the evolutionary history of a temperate gorgonian. Genetica 139:855–869. https://doi.org/10.1007/s10709-011-9589-6

Ballesteros E (2006) Mediterranean coralligenous assemblages: a synthesis of present knowledge. Oceanogr Mar Biol an Annu Rev 44:123–195

Baskett ML, Barnett LAK (2015) The ecological and evolutionary consequences of marine reserves. Annu Rev Ecol Evol Syst 46:49–73. https://doi.org/10.1146/annurev-ecolsys-112414-054424

Benjamini Y, Hochberg Y (1995) Controlling the false discovery rate – A practical and powerful approach to multiple testing. J R Stat Soc B: Stat 57:289–300. https://doi.org/10.1111/j.2517-6161.1995.tb02031.x

Blowes SA, Chase JM, Di Franco A, Frid O, Gotelli NJ, Guidetti P et al (2020) Mediterranean marine protected areas have higher biodiversity via increased evenness, not abundance. J Appl Ecol 57:578–589. https://doi.org/10.1111/1365-2664.13549

Borcard D., Gillet F., Legendre P. (2018) Canonical Ordination. In: Numerical Ecology with R. Use R. Springer, Cham. https://doi.org/10.1007/978-3-319-71404-2_6

Bruckner AW (2010) Quantifying the decline in Corallium rubrum populations: reply to Santangelo & Bramanti (2010). Mar Ecol Prog Ser 418:299–303. https://doi.org/10.3354/meps08898

Cahill AE, De Jode A, Dubois S, Bouzaza Z, Aurelle D, Boissin E et al (2017) A multispecies approach reveals hot spots and cold spots of diversity and connectivity in invertebrate species with contrasting dispersal modes. Mol Ecol 26:6563–6577. https://doi.org/10.1111/mec.14389

Chapuis MP, Estoup A (2007) Microsatellite null alleles and estimation of population differentiation. Mol Biol Evol 24:621–631. https://doi.org/10.1093/molbev/msl191

Chapuis MP, Lecoq M, Michalakis Y, Loiseau A, Sword GA, Piry S, Estoupo A (2008) Do outbreaks affect genetic population structure? A worldwide survey in Locusta migratoria, a pest plagued by microsatellite null alleles. Mol Ecol 17:3640–3653. https://doi.org/10.1111/j.1365-294X.2008.03869.x

Claudet J, Loiseau C, Sostres M, Correspondence MZ (2020) Underprotected marine protected areas in a global biodiversity hotspot. One Earth 2:380–384. https://doi.org/10.1016/j.oneear.2020.03.008

Coll M, Piroddi C, Steenbeek J, Kaschner K, Ben R, Lasram F, Aguzzi J et al (2010) The biodiversity of the mediterranean sea: estimates, patterns, and threats. PLoS ONE 5:e11842. https://doi.org/10.1371/journal.pone.0011842

Costantini F, Gori A, Lopez-González P, Bramanti L, Rossi S, Gili J-M et al (2016) Limited genetic connectivity between gorgonian morphotypes along a depth gradient. PLoS ONE 11:e0160678. https://doi.org/10.1371/journal.pone.0160678

Cramer W, Guiot J, Fader M, Garrabou J, Gattuso J-P, Iglesias A et al (2018) Climate change and interconnected risks to sustainable development in the Mediterranean. Nat Clim Chang 8:972–980. https://doi.org/10.1038/s41558-018-0299-2

Crisci C, Ledoux J-B, Mokhtar-Jamaï K, Bally M, Bensoussan N, Aurelle D et al (2017) Regional and local environmental conditions do not shape the response to warming of a marine habitat-forming species. Sci Rep. https://doi.org/10.1038/s41598-017-05220-4

De Iorio M, Griffiths RC (2004a) Importance sampling on coalescent histories. I. Adv Appl Probab 36:417–433. https://doi.org/10.1239/aap/1086957579

De Iorio M, Griffiths RC (2004b) Importance sampling on coalescent histories. II: Subdivided population models. Adv Appl Probab 36:434–454. https://doi.org/10.1239/aap/1086957580

Díaz S, Demissew S, Carabias J, Joly C, Lonsdale M et al (2015) The IPBES conceptual framework—connecting nature and people. Cur Op Env Sus 14:1–16

Figuerola-Ferrando L, Barreiro A, Montero-Serra I, Pagès-Escolà M, Garrabou J, Linares C, Ledoux J-B (2023) Global patterns and drivers of genetic diversity among marine habitat-forming species. Glob Ecol Biogeogr 32:1218–1229. https://doi.org/10.1111/geb.13685

Foll M, Gaggiotti O (2006) Identifying the environmental factors that determine the genetic structure of populations. Genetics 174:875–891. https://doi.org/10.1534/genetics.106.059451

Gaines SD, White C, Carr MH, Palumbi SR (2010) Designing marine reserve networks for both conservation and fisheries management. Proc Natl Acad Sci USA 107:18286–18293. https://doi.org/10.1073/pnas.0906473107

Garner BA, Hoban S, Luikart G (2020) IUCN red list and the value of integrating genetics. Conserv Genet 21:795–801. https://doi.org/10.1007/s10592-020-01301-6

Garrabou, J., Gómez-Gras, D., Ledoux, J.-B., Linares, C., Bensoussan, N., López-Sendino, P., et al. (2019). Collaborative database to track mass mortality events in the mediterranean sea, Front Mar Sci doi:https://doi.org/10.3389/fmars.2019.00707

Garrabou, J., Ledoux, J.-B., Bensoussan, N., Gómez-Gras, D., and Linares, C. (2021). "Sliding Toward the of Mediterranean Coastal Marine Rocky Ecosystems," in (Springer, Cham), 291–324. doi:https://doi.org/10.1007/978-3-030-71330-0_11.

Gazulla CR, López-Sendino P, Antunes A, Aurelle D, Montero-Serra I, Dominici J-M et al (2021) Demo-genetic approach for the conservation and restoration of a habitat-forming octocoral: the case of red coral, corallium rubrum, in the réserve naturelle de scandola. Front Mar Sci 8:655. https://doi.org/10.3389/fmars.2021.633057

Gómez-Gras D, Linares C, Dornelas M, Madin JS, Brambilla V, Ledoux J et al (2021) Climate change transforms the functional identity of Mediterranean coralligenous assemblages. Ecol Lett 24:1038–1051. https://doi.org/10.1111/ele.13718

Gori A, Rossi S, Berganzo E, Pretus JL, Dale MRT, Gili J-M (2011) Spatial distribution patterns of the gorgonians Eunicella singularis, Paramuricea clavata, and Leptogorgia sarmentosa (Cape of Creus, Northwestern Mediterranean Sea). Mar Biol 158:143–158. https://doi.org/10.1007/s00227-010-1548-8

Guizien K, Viladrich N, Martínez-Quintana Á, Bramanti L (2020) Survive or swim: different relationships between migration potential and larval size in three sympatric Mediterranean octocorals. Sci Rep 10:18096. https://doi.org/10.1038/s41598-020-75099-1

Hoban S, Bruford M, D'Urban Jackson J, Lopes-Fernandes M, Heuertz M, Hohenlohe PA et al (2020) Genetic diversity targets and indicators in the CBD post-2020 Global Biodiversity Framework must be improved. Biol Conserv 248:108654. https://doi.org/10.1016/J.BIOCON.2020.108654

IPCC (2021) *Climate Change 2021: The Physical Science Basis. Contribution of Working Group I to the Sixth Assessment Report of the Intergovernmental Panel on Climate Change*, Cambridge University Press, Cambridge

Jombart T (2008) adegenet: a R package for the multivariate analysis of genetic markers. Bioinformatics 24:1403–1405. https://doi.org/10.1093/bioinformatics/btn129

Jombart T, Devillard S, Balloux F (2010) Discriminant analysis of principal components: a new method for the analysis of genetically structured populations. BMC Genet 11:94. https://doi.org/10.1186/1471-2156-11-94

Jost L (2008) GST and its relatives do not measure differentiation. Mol Ecol 17:4015–4026. https://doi.org/10.1111/j.1365-294X.2008.03887.x

Jost L, Archer F, Flanagan S, Gaggiotti O, Hoban S, Latch E (2018) Differentiation measures for conservation genetics. Evol Appl 11:1139–1148. https://doi.org/10.1111/eva.12590

Lê S, Josse J, Husson F (2008) FactoMineR : An *R* package for multivariate analysis. J Stat Softw 25:1–18. https://doi.org/10.18637/jss.v025.i01

Leblois R, Pudlo P, Néron J, Bertaux F, Reddy Beeravolu C, Vitalis R et al (2014) Maximum-likelihood inference of population size contractions from microsatellite data. Mol Biol Evol 31:2805–2823. https://doi.org/10.1093/molbev/msu212

Ledoux J-B, Mokhtar-Jamaï K, Roby C, Féral J-P, Garrabou J, Aurelle D (2010) Genetic survey of shallow populations of the Mediterranean red coral [*Corallium rubrum* (Linnaeus, 1758)]: new insights into evolutionary processes shaping nuclear diversity and implications for conservation. Mol Ecol 19:675–690. https://doi.org/10.1111/j.1365-294X.2009.04516.x

Ledoux J-B, Frleta-Valić M, Kipson S, Antunes A, Cebrian E, Linares C et al (2018) Postglacial range expansion shaped the spatial genetic structure in a marine habitat-forming species: Implications for conservation plans in the Eastern Adriatic Sea. J Biogeogr 45:2645–2657. https://doi.org/10.1111/jbi.13461

Ledoux J, Frias-Vidal S, Montero-Serra I, Antunes A, Casado Bueno C, Civit S et al (2020) Assessing the impact of population decline on mating system in the overexploited Mediterranean red coral. Aquat Conserv Mar Freshw Ecosyst 30:1149–1159. https://doi.org/10.1002/aqc.3327

Ledoux JB, Ghanem R, Horaud M, López Sendino P, Romero-Soriano V, Antunes A, Bensoussan N, Gómez-Gras D, Linares C, Machordom A, Ocaña O, Templado J, Leblois R, Ben Souissi J, Garrabou J (2021) Gradients of genetic Diversity and Differentiation across the Distribution range of a Mediterranean coral: Patterns, processes and conservation implications. Divers Distrib 27:2104–2123. https://doi.org/10.1111/ddi.13382

Linares C, Coma R, Mariani S, Díaz D, Hereu B, Zabala M (2008) Early life history of the Mediterranean gorgonian Paramuricea clavata: implications for population dynamics. Invertebr Biol 127:1–11. https://doi.org/10.1111/j.1744-7410.2007.00109.x

Linares C, Bianchimani O, Torrents O, Marschal C, Drap P, Garrabou J (2010) Marine Protected Areas and the conservation of long-lived marine invertebrates: The Mediterranean red coral. Mar Ecol Prog Ser 402:69–79. https://doi.org/10.3354/meps08436

Linares C, Doak DF (2010) Forecasting the combined effects of disparate disturbances on the persistence of long-lived gorgonians: a case study of Paramuricea clavata. Mar Ecol Prog Ser 402:59–68. https://doi.org/10.3354/meps08437

Lukoschek V, Riginos C, van Oppen MJH (2016) Congruent patterns of connectivity can inform management for broadcast spawning corals on the Great Barrier Reef. Mol Ecol 25:3065–3080. https://doi.org/10.1111/mec.13649

Magris RA, Andrello M, Pressey RL, Mouillot D, Dalongeville A, Jacobi MN et al (2018) Biologically representative and well-connected marine reserves enhance biodiversity persistence in conservation planning. Conserv Lett 11:e12439. https://doi.org/10.1111/conl.12439

Masmoudi MB, Chaoui L, Topçu NE, Hammami P, Kara MH, Aurelle D (2016) Contrasted levels of genetic diversity in a benthic Mediterranean octocoral: Consequences of different demographic histories? Ecol Evol 6:8665–8678. https://doi.org/10.1002/ece3.2490

Medrano A, Hereu B, Mariani S, Neiva J, Pagès-Escolà M, Paulino C et al (2020) Ecological traits, genetic diversity and regional distribution of the macroalga Treptacantha elegans along the Catalan coast (NW Mediterranean Sea). Sci Rep 10:19219. https://doi.org/10.1038/s41598-020-76066-6

Meirmans PG, Van Tienderen PH (2004) genotype and genodive: two programs for the analysis of genetic diversity of asexual organisms. Mol Ecol Notes 4:792–794. https://doi.org/10.1111/j.1471-8286.2004.00770.x

Mokhtar-Jamaï K, Pascual M, Ledoux J-B, Coma R, Féral J-P, Garrabou J et al (2011) From global to local genetic structuring in the red gorgonian Paramuricea clavata: the interplay between oceanographic conditions and limited larval dispersal. Mol Ecol 20:3291–3305. https://doi.org/10.1111/j.1365-294X.2011.05176.x

Mokhtar-Jamaï K, Coma R, Wang J, Zuberer F, Féral J-P, Aurelle D (2013) Role of evolutionary and ecological factors in the reproductive success and the spatial genetic structure of the temperate gorgonian Paramuricea clavata. Ecol Evol 3:1765–1779. https://doi.org/10.1002/ece3.588

Nei M (1973) Analysis of gene diversity in subdivided populations. Proc Natl Acad Sci 70:3321–3323. https://doi.org/10.1073/pnas.70.12.3321

Nei M (1987) Molecular evolutionary genetics. Columbia University Press, New York, NY

Palumbi SR, Sandifer PA, Allan JD, Beck MW, Fautin DG, Fogarty MJ et al (2009) Managing for ocean biodiversity to sustain marine ecosystem services. Front Ecol Environ 7:204–211. https://doi.org/10.1890/070135

Pérez-Portela, R., Cerro-Gálvez, E., Taboada, S., Tidu, C., Campillo-Campbell, C., et al. Lonely populations in the deep: genetic structure of red gorgonians at the heads of submarine canyons in the north-western Mediterranean Sea. doi:https://doi.org/10.1007/s00338-016-1431-2.

Piry S, Alapetite A, Cornuet J-M, Paetkau D, Baudouin L, Estoup A (2004) GENECLASS2: A software for genetic assignment and first-generation migrant detection. J Hered 95:536–539. https://doi.org/10.1093/jhered/esh074

Pritchard JK, Stephens M, Donnelly P (2000) Inference of population structure using multilocus genotype data. Genetics 155:945–959

Rannala B, Mountain JL (1997) Detecting immigration by using multilocus genotypes. Proc Natl Acad Sci U S A 94:9197–9201. https://doi.org/10.1073/pnas.94.17.9197

Raymond M, Rousset F (1995) An exact test for population differentiation. Evolution 49:1280. https://doi.org/10.2307/2410454

Reynes L, Aurelle D, Chevalier C, Pinazo C, Valero M, Mauger S et al (2021) Population genomics and lagrangian modeling shed light on dispersal events in the mediterranean endemic Ericaria zosteroides (=Cystoseira zosteroides) (Fucales). Front Mar Sci 8:582. https://doi.org/10.3389/fmars.2021.683528

Riquet F, Le Cam S, Fonteneau E, Viard F (2016) Moderate genetic drift is driven by extreme recruitment events in the invasive mollusk Crepidula fornicata. Heredity (edinb) 117:42–50. https://doi.org/10.1038/hdy.2016.24

Rousset F (1997) Genetic differentiation and estimation of gene flow from F-statistics under isolation by distance. Genetics 145:1219–1228

Rousset F (2008) genepop'007: a complete re-implementation of the genepop software for Windows and Linux. Mol Ecol Resour 8:103–106. https://doi.org/10.1111/j.1471-8286.2007.01931.x

Sale PF, Cowen RK, Danilowicz BS, Jones GP, Kritzer JP, Lindeman KC et al (2005) Critical science gaps impede use of no-take fishery reserves. Trends Ecol Evol 20:74–80. https://doi.org/10.1016/j.tree.2004.11.007

Schoener TW (2011) The newest synthesis: understanding the interplay of evolutionary and ecological dynamics. Science 331:426–429. https://doi.org/10.1126/science.1193954

Selkoe K, Toonen R (2011) Marine connectivity: a new look at pelagic larval duration and genetic metrics of dispersal. Mar Ecol Prog Ser 436:291–305. https://doi.org/10.3354/meps09238

Sun JX, Helgason A, Masson G, Ebenesersdóttir SS, Li H, Mallick S, Gnerre S, Patterson N, Kong A, Reich D, Stefansson K (2012) A direct characterization of human mutation based on mi-crosatellites. Nat Genet 44(10):1161–1165

Torrents O, Garrabou J (2011) Fecundity of red coral Corallium rubrum (L.) populations inhabiting in contrasting environmental conditions in the NW Mediterranean. Mar Biol 158:1019–1028. https://doi.org/10.1007/s00227-011-1627-5

Torrents O, Garrabou J, Marschal C, Harmelin JG (2005) Age and size at first reproduction in the commercially exploited red coral Corallium rubrum (L.) in the Marseilles area (France, NW Mediterranean). Biol Conserv 121:391–397. https://doi.org/10.1016/j.biocon.2004.05.010

Tsounis G., Rossi S., Grigg R., Santangelo G., Bramanti L. & Gili J.-M. The Exploitation and Conservation of Precious Corals in Oceanography and Marine Biology: An Annual Review, 2010, 48, 161–212, in R. N. Gibson, R. J. A. Atkinson, and J. D. M. Gordon, Editors Taylor & Francis

Weir BS, Cockerham CC (1984) Estimating F-statistics for the analysis of population structure. Evolution 38:1358. https://doi.org/10.2307/2408641

Authors and Affiliations

Mathilde Horaud[1,2] · Rosana Arizmendi-Meija[1] · Elisabet Nebot-Colomer[3] · Paula López-Sendino[1] · Agostinho Antunes[4,12] · Simon Dellicour[5,6] · Frédérique Viard[7,8] · Raphael Leblois[9] · Cristina Linares[10] · Joaquim Garrabou[1,11] · Jean-Baptiste Ledoux[1,4]

✉ Jean-Baptiste Ledoux
jbaptiste.ledoux@gmail.com

[1] Institut de Ciències del Mar CSIC, Passeig Marítim de La Barceloneta 37-49, 08003 Barcelona, Spain

[2] Norwegian College of Fishery Science, UiT the Arctic University of Norway, Tromsø, Norway

[3] Instituto Español de Oceanográfia - C.O. Baleares (IEO, CSIC), Muelle de Poniente s/n, 07015 Palma de Mallorca, Spain

[4] CIIMAR/CIMAR, Centro Interdisciplinar de Investigação Marinha E Ambiental, Universidade Do Porto, Terminal Do Cruzeiros Do Porto de Leixões, Av. General Norton de Matos, S/N, 4450-208 Porto, Portugal

[5] Spatial Epidemiology Lab (SpELL), Université Libre de Bruxelles, 50 Av. FD Roosevelt, CP160/121050 Bruxelles, Belgium

[6] Department of Microbiology, Immunology and Transplantation, Rega Institute, Laboratory for Clinical and Epidemiological Virology, KU Leuven, University of Leuven, Louvain, Belgium

[7] Sorbonne Université, CNRS, UMR 7144, Station Biologique de Roscoff, Roscoff, France

[8] ISEM, Univ Montpellier, CNRS, IRD, Montpellier, France

[9] CBGP, INRAE, CIRAD, IRD, Montpellier SupAgro, Univ Montpellier, Montpellier, France

[10] Departament de Biologia Evolutiva, Ecologia I Ciències Ambientals, Institut de Recerca de La Biodiversitat, Universitat de Barcelona, Avda. Diagonal 643, 08028 Barcelona, Spain

[11] University of Aix-Marseille, University of Toulon, CNRS, IRD, Mediterranean Institute of Oceanography (MIO), UTM 110, Marseilles, France

[12] Department of Biology, Faculty of Sciences, University of Porto, Rua do Campo Alegre, 4169-007 Porto, Portugal